



# Gas phase dielectric barrier discharge induced reactive species degradation of 2,4-dinitrophenol

Qiong Tang<sup>a,b,c</sup>, Song Lin<sup>b</sup>, Wenju Jiang<sup>b,\*</sup>, T.M. Lim<sup>c</sup>

<sup>a</sup> Department of Chemistry and Life Science, Leshan Normal University, Leshan 614004, PR China

<sup>b</sup> Institute of Architecture and Environment, Sichuan University, Chengdu 610065, PR China

<sup>c</sup> Institute of Environmental Science and Engineering, Nanyang Technology University, Innovation Center, Block 2, Unit 237, 18 Nanyang Drive, Singapore 637723, Singapore

## ARTICLE INFO

### Article history:

Received 13 February 2009

Received in revised form 31 May 2009

Accepted 16 June 2009

### Keywords:

Advanced oxidation processes

Oxidation degradation

2,4-Dinitrophenol

Dielectric barrier discharge

Degradation kinetics

## ABSTRACT

The degradation of 2,4-dinitrophenol (DNP) in aqueous solution by reactive species generated from gas-phase dielectric barrier discharge (DBD) was investigated. The effects of various parameters such as gas flow rate, input power and initial concentration of DNP on the degradation of DNP were further examined. The reactive species generated from the DBD system were measured, and the DNP degradation pathway was analyzed. The results indicated that an aqueous solution of 100 mg L<sup>-1</sup> DNP was 95.0% degraded and 51% of TOC was removed in 60 min treatment at 60 W input power and 7 L min<sup>-1</sup> gas flow rate. The degradation kinetics of DNP was determined to be a pseudo-first-order reaction, which was mainly dependent on the input power, gas flow rate and initial DNP concentrations. The OH· radical was the major reactive species, and played a significant role for the DNP degradation in this study as humid air was used as the gas source.

© 2009 Elsevier B.V. All rights reserved.

## 1. Introduction

Nitrophenols (NPs) are toxic and bio-refractory organic compounds used extensively as raw materials and intermediates in the production of explosives, pharmaceuticals, pesticides, pigments, dyes, wood preservatives and rubber chemicals [1]. It is noteworthy that 2-nitrophenol (2-NP), 4-nitrophenol (4-NP) and 2,4-dinitrophenol (DNP) are listed on US Environmental Protection Agency's (USEPA's) "Priority Pollutants List" and their concentrations in natural water are recommended restricting below 20 ng L<sup>-1</sup> [2]. Therefore, the pollution resulting from NPs discharge into the water environment is considered as one of the general problems.

Due to NPs' high stability and solubility in water, the purification of wastewaters contaminated with NPs by traditional methods is extremely arduous. Research on alternative or additional methods for the oxidative degradation of bio-refractory phenol and its derivatives in aqueous solution is of current interest and has led already to the development of advanced oxidation processes (AOPs) such as ultrasonication [3], electrochemical [4], photocatalytic oxidation [5–7], electrical discharge [8–11] and the combination of them [12–14] at the laboratory scale. Most of these methods focus on hydroxyl radical production directly in the aqueous solution. This is because the hydroxyl radical is a very powerful, non-selective oxidant that has the potential to oxidize bio-refractory organic

compounds. Gas-phase electrical discharge reactors (e.g. dielectric barrier discharge and pulsed corona discharge) have long been used as the most efficient means for ozone generation with clean dry air or pure oxygen [15,16]. More recently, a few studies also found that gas-phase pulsed corona discharge could be an effective way to generate OH· radicals with air containing water vapor [17–20]. Most importantly, the density of OH· radicals generated in the discharge zone could be several times higher than that of ozone [18,21,22]. However, there was no study of degradation pollutants in the aqueous solution by gas phase electric discharge process with air containing water vapor.

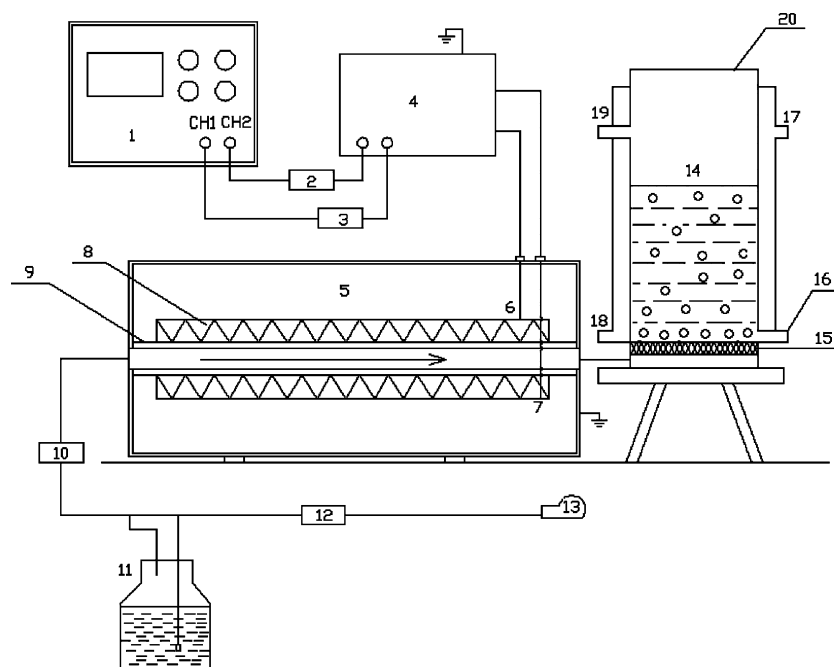
The current research aimed at producing the reactive species (e.g. OH·, H<sub>2</sub>O<sub>2</sub>, O<sub>3</sub>) by using a gas-phase dielectric barrier discharge (DBD) process with air containing water vapor as the gas source. Subsequently the reactive species were diffused into aqueous solution to oxidize the pollutants. 2,4-Dinitrophenol (DNP) was used as the target compound to test the effectiveness of the DBD system.

## 2. Materials and methods

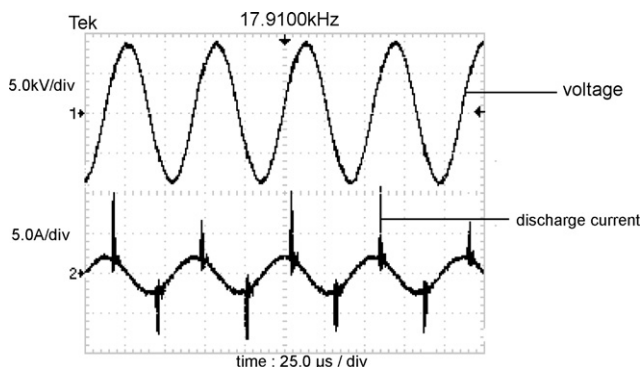
### 2.1. Experimental set-up

Fig. 1 shows the schematic diagram of the experimental set-up, which consisted of a DBD reactor to produce reactive species, an alternating current (AC) high voltage power supply, a gas supply and a reactor vessel containing the DNP solution. The DBD reactor was comprised of two stainless steel electrodes encased by outer stainless steel container, and two quartz dielectrics were installed

\* Corresponding author. Tel.: +86 28 85403016; fax: +86 28 85405613.  
E-mail address: [wenjujiang@scu.edu.cn](mailto:wenjujiang@scu.edu.cn) (W. Jiang).



**Fig. 1.** Schematic diagram of the experimental set-up. (1) Oscilloscope; (2) current probe; (3) voltage probe; (4) AC high voltage power (5) DBD reactor; (6) high voltage electrode; (7) ground electrode; (8) stainless steel electrodes; (9) quartzes dielectric; (10) humidity analyzer; (11) humidifier; (12) gas flow rate meter; (13) gas pump; (14) reactor vessel; (15) porous aerated plate; (16) sampling; (17) cooling water outlet; (18) cooling water inlet; (19) wastewater inlet; (20) gas outlet.



**Fig. 2.** Typical waveforms of the applied voltage and discharge current.

on the surface of the electrodes to produce barrier discharge. The gas spacing between the two dielectrics was 2 mm, between which an AC high voltage was applied. The acrylic reactor vessel had an inner diameter of 80 mm and a height of 300 mm, and was fitted with a water-jacket for temperature control. The reactor vessel was connected to the DBD reactor by using a length of 5 cm and 1/8 in. diameter stainless steel tubing. An annular porous diffuser was placed at the bottom of reactor vessel to distribute gases containing reactive species. The feed gas was passed through a water bubbler by an air pump to increase the humidity, then into the DBD reactor. The flow rate and relative humidity (RH) of the gas were monitored with a gas flow meter, and a humidity analyzer, respectively. The applied voltage and discharge current wave of the DBD reactor were recorded using a digital storage oscilloscope (TDS 1001B, Tektronix). Fig. 2 shows a typical waveform of the peak-to-peak voltage ( $V_{pp}$ ) and discharge current.

## 2.2. Experimental procedures

2,4-Dinitrophenol (DNP) (99%) was obtained from Sigma–Aldrich, and was used without further purification. Aqueous solutions containing 50–200 mg L<sup>-1</sup> DNP were prepared

with Milli-Q water. 500 mL of the DNP solution was put into the reactor vessel to be degraded by the reactive species generated from the DBD system. Humid air with an RH of 100% (25 °C) was fed into the DBD system by passing air through a water bubbler, and the gas flow rate was varied in the range of 3–8 L min<sup>-1</sup>. Temperature in the reactor was kept around 25 °C. The AC high voltage applied to the DBD system was varied from 18 kV to 24 kV (peak value). The duration of each experiment was kept at 60 min.

Samples were taken from the reactor vessel at regular intervals for analyses. DNP concentrations were determined by a high-pressure liquid chromatograph (HPLC) (WATERS 2695, separations module: XBridge C<sub>18</sub> column) with a multiple wavelength UV diode array detector (WATERS 2996). The determination wavelength was set at 360 nm. The mobile phase used consisted of 70% methanol and 30% water and the column temperature was maintained at 30 °C. Spectrums of samples were obtained by an UV–vis spectrophotometer (Jasco V-550) with Milli-Q water as the blank. Total organic carbon (TOC) was analyzed using a Shimadzu TOC-Vcph analyzer after samples were filtered through 0.45 μm PTFE membrane. The pH of the solution was measured with an YSI pH100 portable pH meter.

The HPLC (WATERS 2695, separations module, XBridge C<sub>18</sub> column) with a multiple wavelength UV diode array detector (WATERS 2996) was also used to determine the concentrations of OH· radicals, following the dimethyl sulfoxide trapping method developed by Chao Tai [23]. In this method, the concentration of OH· radicals is indirectly measured by the concentration of 2,4-dinitrophenyl-hydrazone (DNPho), which is formed by the reaction between 2,4-dinitrophenyl-hydrazine (DNPH) and the adduct of OH· radicals and dimethyl sulfoxide (DMSO). The concentrations of hydrogen peroxide and ozone in the solution were determined by the potassium titanium (IV) oxalate method and potassium indigotrisulfonate method, respectively, using a Jasco V-550 UV–vis spectrometer (Japan) [24,25]. The concentrations of NO<sub>2</sub><sup>-</sup> and NO<sub>3</sub><sup>-</sup> were measured by an ion chromatography (Dionex ICS-3000, Singapore) coupled with an AS-19 non-suppressor column (4.6 mm × 150 mm) and a CDD-10A VP conductivity detector. A KOH eluent solution (10 mmol L<sup>-1</sup> for first 10 min and then raised grad-

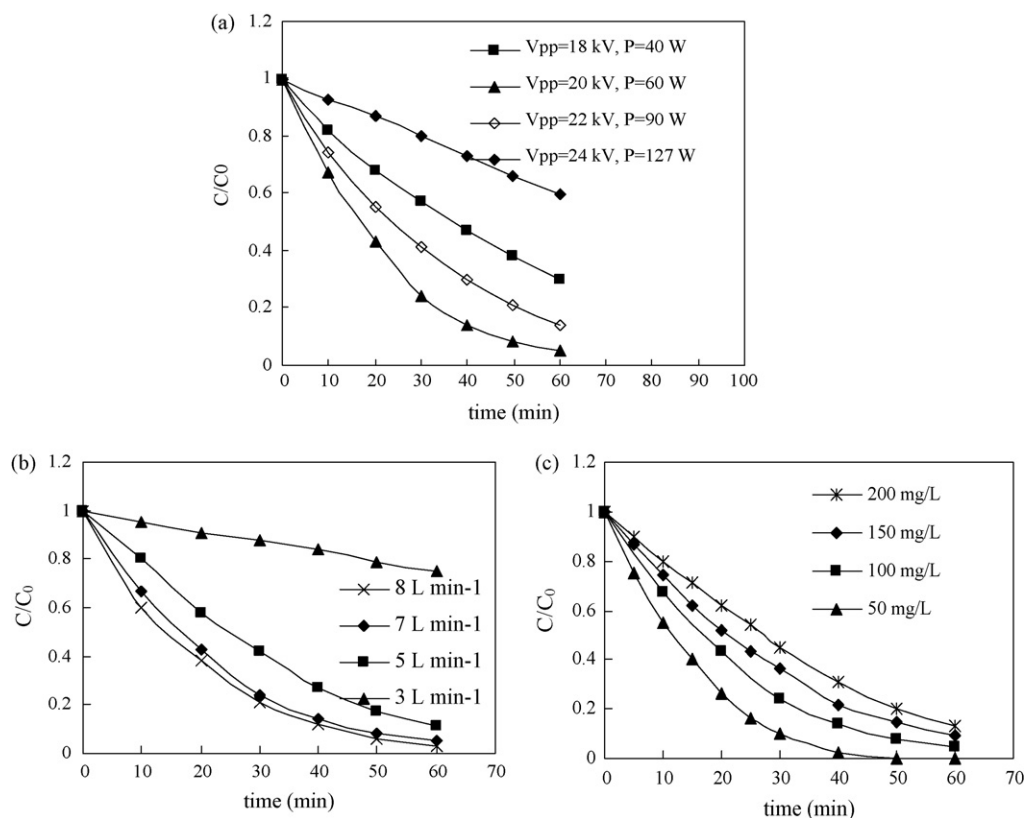


**Fig. 3.** Effect of operational conditions on degradation of DNP: (a) effect of input power: initial DNP concentration of  $100 \text{ mg L}^{-1}$ ; gas flow rate of  $7 \text{ L min}^{-1}$ , (b) effect of inlet gas flow rate: initial DNP concentration of  $100 \text{ mg L}^{-1}$ ; input power of  $60 \text{ W}$ , and (c) effect of concentration of DNP: input power of  $60 \text{ W}$ , gas flow rate of  $7 \text{ L min}^{-1}$ .

ually to  $45 \text{ mmol L}^{-1}$  followed  $15 \text{ min}$ ) was pumped at a flow rate of  $1.0 \text{ ml min}^{-1}$ .

### 3. Results and discussion

#### 3.1. Effect of initial conditions on the degradation of DCP

The effect of different initial conditions, i.e. input power, gas flow rate and initial DNP concentration were discussed in this section. Experimental results (Fig. 3) showed that DNP concentrations decreased with the treatment time in a near exponential fashion. A pseudo-first-order kinetics was used to describe the removal rates with respect to the DNP initial concentrations:

$$\ln\left(\frac{C}{C_0}\right) = -kt \quad (3)$$

where  $C_0$  and  $C$  are the concentrations of DNP at times 0 and  $t$  ( $\text{mg L}^{-1}$ ), respectively,  $t$  is the treatment time (min), and  $k$  is

the pseudo-first-order rate constant ( $\text{min}^{-1}$ ) presented in Table 1, which showed great difference under various experimental conditions.

#### 3.1.1. Effect of input power

Fig. 3a shows the degradation of DNP under different input power at an initial concentration of  $100 \text{ mg L}^{-1}$  and a gas flow rate of  $7 \text{ L min}^{-1}$ . The degradation rate of DNP increased with increasing input power initially, and then decreased with further increasing above  $60 \text{ W}$ . The pseudo-first-order rate constants ( $k$ ) rose from  $0.0197 \text{ min}^{-1}$  to  $0.0513 \text{ min}^{-1}$  corresponding to the input power of  $40 \text{ W}$  and  $60 \text{ W}$ , respectively, but reduced to  $0.0086 \text{ min}^{-1}$  under the input power of  $127 \text{ W}$  (Table 1). When the input power was higher than  $127 \text{ W}$ , the degradation of DNP can hardly be observed.

The input power has a significant effect on the active species production. As the input power increases, electrons gain more energy in the electric field and induce more ionization of oxy-

**Table 1**  
Pseudo-first-order rate constants of obtained under various operation parameters applied in the treatment.

Operation parameters			Pseudo-first-order ( $k$ ) ( $\text{min}^{-1}$ )	$R^2$	$n$
Initial concentration ( $C_0$ ) ( $\text{mg L}^{-1}$ )	$P$ (W)	Gas flow rate ( $\text{L min}^{-1}$ )			
50	60	7	0.0784	0.9870	6
100	60	7	0.0513	0.9973	6
150	60	7	0.0395	0.9953	6
200	60	7	0.0342	0.9832	6
100	40	7	0.0197	0.9982	6
100	90	7	0.0322	0.9964	6
100	127	7	0.0086	0.9944	6
100	60	3	0.0047	0.9939	6
100	60	5	0.0374	0.9872	6
100	60	8	0.0581	0.9945	6

gen and water molecules by collision [26]. The increase of active species formation is likely to be responsible for the significantly higher degradation rates under high input powers. However, when the input power is increased to a level, UV radiation can occur which will affect the discharge mode of the DBD reactor, and result in the reduction of micro-discharge frequency. Moreover,  $\text{NO}_x$  production can be enhanced under excessive power, which will consume oxygen atoms and accelerate their recombination [16]. Therefore the formation rate of reactive species might decrease with increasing input power when the input power was set beyond 60 W in this study, correspondingly the degradation rate of DNP decreased with increasing input power from 60 W to 127 W.

### 3.1.2. Effect of inlet gas flow rate

Various gas flow rates were applied to the DBD reactor to study their effect on the degradation of DNP. The results are shown in Fig. 3b and Table 1. It was observed that increasing the gas flow rate from  $3 \text{ L min}^{-1}$  to  $8 \text{ L min}^{-1}$  improved the degradation of DNP. The rate constants rose from  $0.0047 \text{ min}^{-1}$  to  $0.0581 \text{ min}^{-1}$  under gas flow rates of  $3 \text{ L min}^{-1}$  and  $8 \text{ L min}^{-1}$ , respectively.

Gas flow rate affects significantly the quantity of gas molecules present in the DBD reactor, thereby the pressure within. The pressure in the DBD reactor causes the change in the energy density and the transferred charge, and then affects the number of micro-discharges occurring per unit of electrode area. This finally determines the abundance of gas molecules broken down and the quantities of active species generated [16]. On the other hand, gas flow rate affects the residence time of the gas in the reactor and the reaction time of active species (such as  $\text{OH}\cdot$  radical,  $\text{O}_3$ ) with pollutant molecules, which finally determines the utilization ratio of the active species [26].

With the gas flow rate increase, therefore, more gas molecules will pass through the DBD reactor and break down by collision with energetic electrons within the same time span, and hence more reactive species will be generated. Moreover, the time required for the gas molecules to reach the reactor vessel is reduced with higher gas flow rate, resulting in more reactive species reacting with DNP within their lifetime, i.e. higher utilization ratio of reactive species. This is likely to be the reason why in this test the degradation rate of DNP increased with increasing gas flow rate. However, increase of gas flow rate in turn reduces the residence time and reaction time of the reactive species with the pollutants. This might explain the fact that the increase of degradation rate was much less pronounced when the flow rate was further increased from  $7 \text{ L min}^{-1}$  to  $8 \text{ L min}^{-1}$ .

### 3.1.3. Effect of concentration of DNP

Fig. 3c shows the effect of initial concentrations of DNP on the degradation of DNP. The rate constants decreased with increasing initial concentrations of DNP, i.e. it dropped from  $0.0784 \text{ min}^{-1}$  to  $0.0342 \text{ min}^{-1}$  when the initial DNP concentration increased from  $50 \text{ mg L}^{-1}$  to  $200 \text{ mg L}^{-1}$  (Table 1). Higher initial concentration means more DNP molecules present in the solution while the amount of reactive species generated remain the same. Therefore when the initial concentration increased, the competition between DNP molecules and/or its intermediates for the reactive species may become more intensive as the reactive species were non-selective. Accordingly, lower degradation rates of DNP were obtained under higher initial concentrations.

## 3.2. Mineralization and final products of degradation of DNP

Mineralization of DNP in this section was studied by change in UV-vis spectra,  $\text{NO}_3^-$  and  $\text{NO}_2^-$  evolution, and also TOC removal.

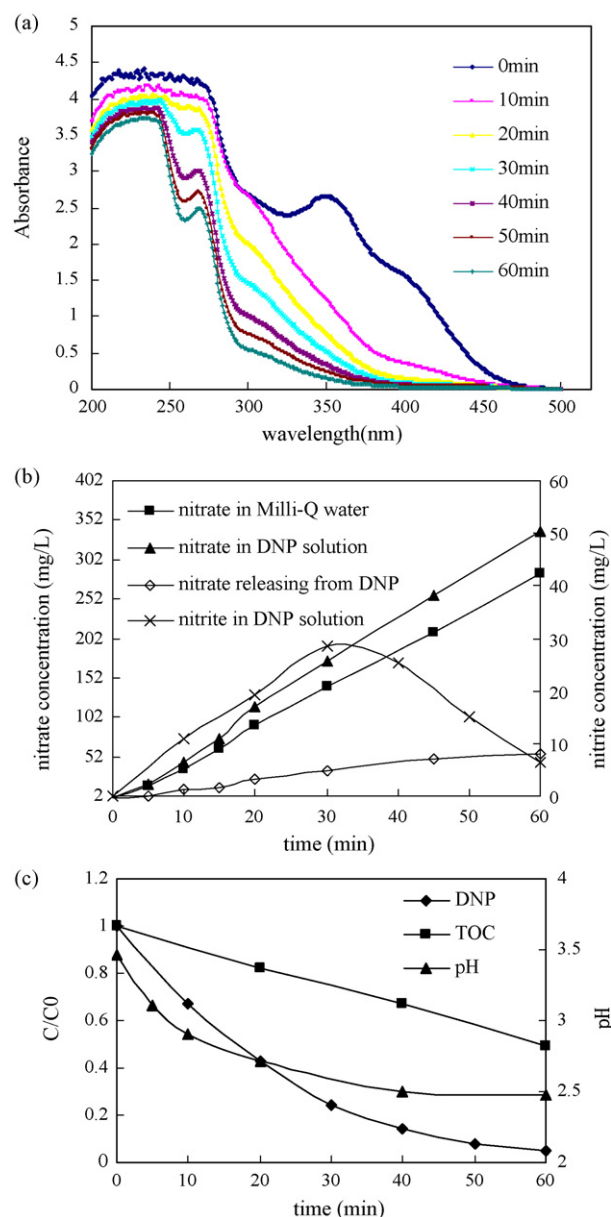


Fig. 4. (a) UV-vis spectrum along with reaction time, (b) evolution of  $\text{NO}_3^-$  and  $\text{NO}_2^-$  along with treatment time, and (c) evolution of DNP, TOC and pH along with treatment time. (Initial condition was input power 60 W; gas flow rate  $7 \text{ L min}^{-1}$ ; initial DNP  $100 \text{ mg/L}$ .)

### 3.2.1. UV-vis absorption spectra

The change in the UV-vis absorption spectra of DNP solution during oxidation degradation processes has been shown in Fig. 4a. As can be seen from Fig. 4a, the absorption peaks at 360 nm disappeared quickly following the treatment. Moreover, the whole absorption band diminished gradually with treatment time, and a peak at 269 nm was obviously observed then decreased gradually from 30 min to 60 min. All above mentioned results indicated the degradation of DNP and the formation of intermediates with low molecular weight. Along with the treatment time, further degradation of intermediates was also obtained.

### 3.2.2. The Formation of $\text{NO}_3^-$ and $\text{NO}_2^-$

To obtain better understanding of DNP mineralization by reactive species generated,  $\text{NO}_3^-$  and  $\text{NO}_2^-$  ions were monitored during the treatment process. Milli-Q water was subjected to DBD treatment for 60 min under the same conditions. The concentration of



**Table 2**

Formation rate of reactive species at the gas source of humid air (RH 100%), input power of 60 W and gas flow rate of 7 L min<sup>-1</sup>.

Reactive species	Rate constant $k$ (mol L <sup>-1</sup> min <sup>-1</sup> )
Hydroxyl radical	$3.56 \times 10^{-6}$
Hydrogen peroxide	$1.55 \times 10^{-7}$
Ozone	$2.12 \times 10^{-7}$

NO<sub>3</sub><sup>-</sup> and NO<sub>2</sub><sup>-</sup> releasing from DNP were calculated by subtracting the concentration in milli-Q water from the concentration in DNP solution, respectively. As the dissolving of these acidic ions can be expected to lower the pH value, pH of the solutions was also measured as an indication of the mineralization progress. The results are shown in Fig. 4b and c. It can be seen that The NO<sub>2</sub><sup>-</sup> in milli-Q water was undetectable and its concentration in DNP solution declined after an initial increase, probably due to its oxidation to form NO<sub>3</sub><sup>-</sup>. While the concentration of NO<sub>3</sub><sup>-</sup> in DNP solution and milli-Q water both increased gradually until the end of the treatment. Moreover, the concentration of NO<sub>3</sub><sup>-</sup> releasing from DNP increased slowly initial 20 min, and then the rate increased gradually. These results indicated that the NO<sub>2</sub><sup>-</sup> mainly results from the degradation of DNP, the nitrogen molecules in the gas phase were mostly oxidized into NO<sub>2</sub> before being dissolved into solution. Moreover, NO<sub>2</sub><sup>-</sup> was formed first when the nitrogen-to-carbon single bond (-N-C-) of the DNP was broken down and then was oxidized into NO<sub>3</sub><sup>-</sup>. At 60 min, the total concentration of N-containing products (NO<sub>2</sub><sup>-</sup> and NO<sub>3</sub><sup>-</sup>) releasing from DNP was approximately 63.32 mg/L (calculated as NO<sub>3</sub><sup>-</sup>), which is close to stoichiometric value of 67.39 mg/L, indicating that nitrogen-to-carbon single bond (-N-C-) of the DNP was mostly broken down and converted into NO<sub>2</sub><sup>-</sup> and NO<sub>3</sub><sup>-</sup> at 60 min.

From the Fig. 4c, the pH dropped quickly in the early part of the process from the initial 3.46. After 20 min, the pH decreased to 2.71. Further, it slowly decreased until the end of the treatment, and reached the value of 2.48 at 60 min. The drop in the pH is probably explained by the formation of strong acids as a consequence of oxidation of the DNP and nitrogen in air.

### 3.2.3. Extent of TOC removal and pH change

The change in UV-vis absorption spectra and the formation of NO<sub>2</sub><sup>-</sup> and NO<sub>3</sub><sup>-</sup> only reflect the extent of degradation of DNP but do not reflect the mineralization extent of DNP. The TOC values have been related to the total concentration of organic in the solution and the decrease of TOC can reflect the degree of mineralization as a function of residence time. Therefore the TOC removal and the results are shown in Fig. 4c. From Fig. 4c, about 95.0% degradation of DNP was achieved at 60 min, while only 51% TOC was removed indicating slower mineralization being obtained. Therefore though the nitryl radical (-NO<sub>2</sub>) was mostly released from the benzene ring at 60 min the DNP was not mineralized completely to convert into the CO<sub>2</sub> and H<sub>2</sub>O. Some other intermediate products with low molecular weight were formed. This is consistent with the UV-vis absorption spectra.

## 3.3. Analysis of DNP degradation pathways in the DBD system

### 3.3.1. Formation of reactive species in solutions

The initiation concentrations of OH· radical, hydrogen peroxide and ozone in the solutions were measured and the formation rates were calculated, and the results are shown in Fig. 5 and Table 2. A nearly linear increase in concentrations of OH· radical and hydrogen peroxide was observed with the treatment time, indicating that the formation of OH· radical and hydrogen peroxide in solution is a zero order reaction. However the concentration of ozone in solution increased fast within the initial 5 min, then the formation rate

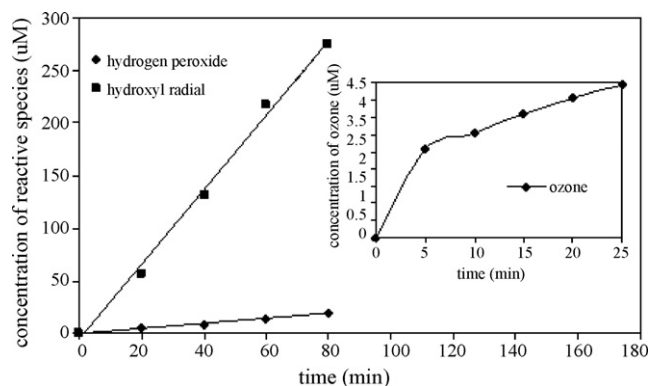
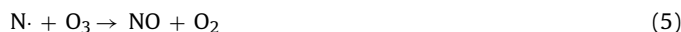


**Fig. 5.** Formation rate of reactive species in solution at an input power of 60 W, gas source of humid air (RH 100%) and gas flow rate of 7 L min<sup>-1</sup>.

slowed down from 5 min to 25 min. As shown in Table 2, it was also discovered that the OH· radical was the major reactive species and its concentration is several times greater than that of ozone and hydrogen peroxide.

Earlier studies found that the composition of the gas source have a significant effect on the generation of reactive species [18,22]. Lukes et al. reported that when air containing water vapor was used, the presence of water and N<sub>2</sub> molecules in humid air could inhibit O<sub>3</sub> production and enhance OH· radical formation through the following reactions [27]:



Therefore, OH· radical was the major reactive species and its concentration was several times higher than that of ozone and hydrogen peroxide as humid air was used as the gas source in this study.

### 3.3.2. Analysis of possible pathways

From Fig. 5 and Table 2, the OH· radical was the major reactive species and its concentration was several times higher than that of ozone and hydrogen peroxide. Moreover, OH· radical has much higher oxidation potential than O<sub>3</sub> and many studies have shown that OH· radical reacted with most pollutants 10<sup>6</sup> to 10<sup>9</sup> times faster than that ozone [28,29]. Therefore the effectiveness of oxidation process for the DNP is associated with OH· radical in this study.

The tentative reaction pathway for degradation of NPs by OH· radical has been studied by Kavitha et al. [12] and Lukes and Locke [30] and similar results were obtained. OH· radical is strongly electrophilic, and would attack aromatic ring firstly from the carbon atom with highest electron density. This character of OH· radical led to formation of hydroxylated nitrophenols firstly when it attacked the nitrophenols. If these primary hydroxylated nitrophenols were further attacked by OH· radical, the aromatic ring would open; meanwhile, a series of aliphatic acids, oxalic acid, formic acid and acetic acid would be formed. These acids could further react with OH· radical, and produce ultimate products: CO<sub>2</sub> and H<sub>2</sub>O. In the process, -NO<sub>2</sub> group could be easily removed from the aromatic ring by direct attack of OH· radical, resulting in formation of NO<sub>3</sub><sup>-</sup> in

**Table 3**  
Energy efficiency of advanced oxidation processes treatment for phenol.

Discharge type	Initial conc. (mg L <sup>-1</sup> )	Vol. (L)	P (W)	Time (min)	C (%)	Energy efficiency (g kWh <sup>-1</sup> )	Ref.
Dielectric barrier humid air used	DNP: 100	0.5	60	40	86	1.075	This paper
Dielectric barrier humid air used	DNP: 200	0.5	60	60	87	1.45	This paper
Dielectric barrier in water	DNP: 4.6	0.3	150	1	83.6	0.46	[10]
Corona in water	Phenol: 46					0.35	[9]
Spark in water	Phenol: 50					0.77	[9]
Ultrasound in a Fenton system	DCP: 100	0.4	385	30	86.5	0.18	[14]
Ultrasound O <sub>3</sub> additive	DNP: 20	0.05	44	50	100	0.27	[13]

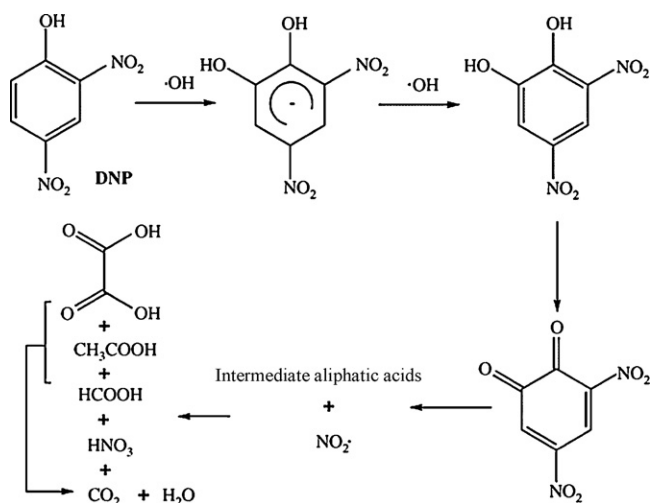


**Fig. 6.** The proposed mechanism of DNP degradation by DBD system.

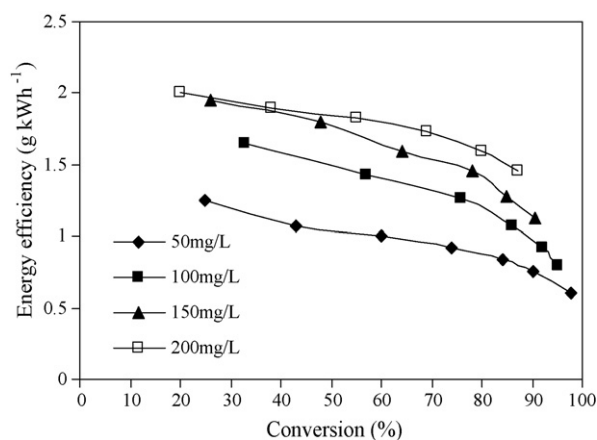


**Fig. 7.** Energy efficiency for DNP degradation as a function of the conversion at various initial DNP concentrations.

the oxidizing media [30]. This can also be supported by the formation of NO<sub>3</sub><sup>-</sup> and NO<sub>2</sub><sup>-</sup> from Section 3.2.2 in this study. Therefore, the possible primary mechanism of DNP degradation by present DBD system was proposed and shown in Fig. 6 [10].

### 3.4. Energy efficiency

The above investigation focuses on the reaction mechanisms and improvement of removal. However, in practice, energy efficiency is an important factor. The energy efficiencies of present DBD system for various initial DNP concentrations are given in Fig. 7 and Table 3. The results showed that higher energy efficiency was obtained under higher initial DNP concentration and lower degradation rate. The results by other authors for phenol and its derivative degradation are also given in Table 3. Lower value of the energy efficiency

for phenol degradation in spark discharge system (0.77 g kWh<sup>-1</sup>) was obtained by Sun et al. [9]. Much lower efficiencies were found in the ultrasound systems, where the energy efficiency for DCP and DNP degradation was 0.18 g kWh<sup>-1</sup> and 0.27 g kWh<sup>-1</sup>, respectively [13,14]. Therefore, the energy efficiency is dependent on reactor types, the target compound and the initial concentration of the compound. Most importantly, the energy efficiency in this study was higher than those obtained in other lab scale studies, and it could be further improved in the process of scaling-up.

### 4. Conclusions

In this work, the degradation of DNP in aqueous solution and formation of reactive species by DBD system was investigated. The possible degradation pathway of DNP was analyzed. The conclusion can be made as follows:

- (1) The present DBD system is an effective technology for the treatment of DNP solution, and the degradation was almost completed within 60 min with initial DNP concentration of 100 mg L<sup>-1</sup> at 60 W input power and 7 L min<sup>-1</sup> gas flow rate. Approximately 51% of the initial TOC was removed after 60 min treatment. The degradation of DNP followed pseudo-first-order kinetics, which was dependent on operating conditions such as input power, gas flow rate, and initial DNP concentration. Compared with other electric discharge in water, the energy efficiency in present system was improved.
- (2) The reactive species such as OH· radical, ozone and hydrogen peroxide can be generated by the present DBD system. The OH· radical was the major reactive species and its concentration was several times greater than that of ozone and hydrogen peroxide as humid air was used as the gas source in this study, and played a significant role for the DNP degradation.

### References

- [1] V. Uberoi, S.K. Bhattacharya, Toxicity and degradability of nitrophenols in anaerobic systems, *Water Environ. Res.* 69 (1997) 146–156.
- [2] EPA, July 2002, <http://www.scorecard.org>.
- [3] Z.B. Guo, Z. Zheng, S.R. Zheng, W.Y. Hu, R. Feng, Effect of various sono-oxidation parameters on the removal of aqueous 2,4-dinitrophenol, *Ultrason. Sonochem.* 12 (2005) 461–465.
- [4] H. Wang, J.L. Wang, Electrochemical degradation of 2,4-dichlorophenol on a palladium modified gas-diffusion electrode, *Electrochim. Acta* 53 (2008) 6402–6409.
- [5] H.C. Liang, X.Z. Li, Y.H. Yang, K.H. Sze, Effects of dissolved oxygen, pH, and anions on the 2,3-dichlorophenol degradation by photocatalytic reaction with anodic TiO<sub>2</sub> nanotube films, *Chemosphere* 73 (2008) 805–812.
- [6] L. Wu, A.M. Li, G.D. Gao, Z.H. Fei, S.R. Xu, Q.X. Zhang, Efficient photodegradation of 2,4-dichlorophenol in aqueous solution catalyzed by polydivinylbenzene-supported zinc phthalocyanine, *J. Mol. Catal. A: Chem.* 269 (2007) 183–189.
- [7] K. Nakano, E. Obuchi, S. Takagi, R. Yamamoto, T. Tanizaki, M. Taketomi, M. Eguchi, K. Ichida, M. Suzuki, A. Hashimoto, Photocatalytic treatment of water containing dinitrophenol and city water over TiO<sub>2</sub>/SiO<sub>2</sub>, *Sep. Purif. Technol.* 34 (2004) 67–72.
- [8] A.K. Sharma, G.B. Josephson, D.M. Camaioni, S.C. Goheen, Destruction of pentachlorophenol using glow discharge plasma process, *Environ. Sci. Technol.* 34 (2000) 2267–2272.
- [9] B. Sun, M. Sato, J.S. Clements, Oxidative processes occurring when pulsed high voltage discharges degrade phenol in aqueous solution, *Environ. Sci. Technol.* 34 (2000) 509–513.

- [10] J.B. Zhang, Z. Zheng, Y.N. Zhang, J.W. Feng, J.H. Li, Low-temperature plasma-induced degradation of aqueous 2,4-dinitrophenol, *J. Hazard. Mater.* 154 (2008) 506–512.
- [11] J.Z. Gao, Y.J. Liu, W. Yang, L.M. Pu, J. Yu, Q.F. Lu, Oxidative degradation of phenol in aqueous electrolyte induced by plasma from a direct glow discharge, *Plasma Sour. Sci. Technol.* 12 (2003) 533–538.
- [12] V. Kavitha, K. Palanivelu, Degradation of nitrophenols by Fenton and photo-Fenton processes, *J. Photochem. Photobiol. A: Chem.* 170 (2005) 83–95.
- [13] Z.B. Guo, R. Feng, J.H. Li, Z. Zheng, Y.F. Zheng, Degradation of 2,4-dinitrophenol by combining sonolysis and different additives, *J. Hazard. Mater.* 158 (2008) 164–169.
- [14] T. Zhou, Y.Z. Li, F.S. Wong, X.H. Lu, Enhanced degradation of 2,4-dichlorophenol by ultrasound in a new Fenton like system (Fe/EDTA) at ambient circumstance, *Ultrason. Sonochem.* 15 (2008) 782–790.
- [15] M. Simek, M. Clupek, Efficiency of ozone production by pulsed positive corona discharge in synthetic air, *J. Phys. D: Appl. Phys.* 35 (2002) 1171–1175.
- [16] U. Kogelschatz, Dielectric-barrier discharges: their history, discharge physics, and industrial applications, *Plasma Chem. Plasma Process.* 23 (2003) 1–46.
- [17] D.N. Shin, C.W. Park, J.W. Hahn, Detection of OH ( $A^2P^+$ ) and O ( $^1D$ ) emission spectrum generated in a pulsed corona plasma, *Bull. Korean Chem. Soc.* 21 (2000) 228–232.
- [18] R. Ono, T. Oda, Dynamics of ozone and OH radicals generated by pulsed corona discharge in humid-air flow reactor measured by laser spectroscopy, *J. Appl. Phys.* 93 (2003) 5876–5882.
- [19] F. Tochikubo, S. Uchida, T. Watanabe, Study on decay characteristics of OH radical density in pulsed discharge in Ar/H<sub>2</sub>O, *Jpn. J. Appl. Phys. Part 1* 43 (2004) 315–320.
- [20] R. Ono, T. Oda, Measurement of hydroxyl radicals in an atmospheric pressure discharge plasma by using laser-induced fluorescence, *IEEE Trans. Ind. Appl.* 36 (2000) 82–86.
- [21] R. Ono, T. Oda, Measurement of hydroxyl radicals in pulsed corona discharge, *J. Electrostat.* 55 (2002) 333–342.
- [22] J. Kornev, N. Yavorovsky, S. Preis, M. Khaskelberg, U. Isaev, B.-N. Chen, Generation of active oxidant species by pulsed dielectric barrier discharge in water–air mixtures, *Ozone Sci. Eng.* 28 (2006) 207–215.
- [23] T. Chao, F.P. Jin, F.L. Jing, G.B. Jiang, Z. Hong, Determination of hydroxyl radicals in advanced oxidation processes with dimethyl sulfoxide trapping and liquid chromatography, *Anal. Chim. Acta* 527 (2004) 73–80.
- [24] R.M. Sellers, Spectrophotometric determination of hydrogen peroxide using potassium titanium (IV) oxalate, *Analyst* 105 (1980) 950–954.
- [25] H. Bader, J. Hoigne, Determination of ozone in water by the indigo method, *Water Res.* 15 (1981) 449–456.
- [26] R.B. Zhang, C. Zhang, X.X. Cheng, L.M. Wang, Y. Wu, Z.C. Guan, Kinetics of decolorization of azo dye by bipolar pulsed barrier discharge in a three-phase discharge plasma reactor, *J. Hazard. Mater.* 142 (2007) 105–110.
- [27] P. Lukes, M. Clupek, V. Babicky, V. Janda, P. Sunka, Generation of ozone by pulsed corona discharge over water surface in hybrid gas–liquid electrical discharge reactor, *J. Phys. D: Appl. Phys.* 38 (2005) 409–416.
- [28] W.R. Haag, C.C. Yao, Rate constants of reaction of hydroxyl radicals with several drinking water contaminants, *Environ. Sci. Technol.* 26 (1992) 1005–1013.
- [29] C.C. Yao, W.R. Haag, Rate constants for direct reaction of ozone with several drinking water contaminants, *Water Res.* 25 (1991) 761–773.
- [30] P. Lukes, B.R. Locke, Degradation of substituted phenols in a hybrid gas–liquid electrical discharge reactor, *Ind. Eng. Chem. Res.* 44 (2005) 2921–2930.